2025 IMEKO TC26 International Conference on
Metrology for Archaeology and Cultural Heritage
Bergamo, Italy, October 15-17, 2025

Multi-Technique Characterization of Mortars from Gammarth Villa (Tunisia)

Manel Górriz i Villar[1], Mirco Ramacciotti[1], Iván Fumadó Ortega[1], Hamden Ben Romdhane[2], Ángel Morales-Rubio[3], Gianni Gallello[1,4]

[1] Dep. of Prehistory, Archaeology and Ancient History, University of Valencia, Valencia, Spain.
[2] Institut National du Patrimoine, Tunis, Tunisia.
[3] Dep. of Analytical Chemistry, University of Valencia, Burjassot, Spain.
[4] University Institute of Materials Science (ICMUV), University of Valencia, Paterna, Spain.

Abstract **– This study presents the multi-technique characterization of lime mortars from the Villa of Gammarth, an archaeological site north of Carthage (Tunisia). Sixteen samples from wall renders, structural joints, and waterproof coatings were analyzed using attenuated total reflectance infrared spectroscopy, portable X-ray fluorescence, and inductively coupled plasma mass spectrometry. The analysis focused on major, minor, and trace elements, including Rare Earth Elements, and molecular signatures of the mortars. Results reveal different compositional groups based on chemical characteristics. Multivariate statistics applied to elemental data identified chemical clusters and outliers, suggesting different construction events or undocumented restorations. This integrated approach proves effective for interpreting construction technologies, raw material changes, and surface interventions, especially in sites with poor stratigraphic resolution. The Gammarth Villa case contributes valuable archaeometric data on ancient North African building practices.**

I. INTRODUCTION

The analysis of ancient lime mortars is crucial in the study of built heritage, offering key insights into construction technologies, raw material procurement, and architectural transformations over time. Compositional variability in mortars may reflect building sequences, functional differentiation, or later interventions. This is especially relevant in sites with limited stratigraphic resolution, where material analysis often provides the primary means of reconstructing diachronic processes [1-4].

Multi-technique approaches have proven effective in this regard. Elemental methods such as portable X-ray fluorescence (pXRF) and inductively coupled plasma mass spectrometry (ICP-MS) enable precise quantification of major, minor, and trace elements, including rare earth elements (REEs), which serve as geochemical markers of provenance and technological selection [5, 6]. Attenuated total reflectance infrared spectroscopy (ATR-IR) allows the identification of minerals, and organic or hydraulic phases, complementing elemental data [7-9]. Multivariate statistics, especially principal component analysis (PCA), allow for the systematic interpretation of complex datasets, facilitating the identification of compositional clusters and outliers indicative of distinct building phases, recipes or repair episodes [10, 11].

The present study applies a multi-analytical strategy combining ATR-IR, pXRF, and ICP-MS to a set of mortars from the Villa of Gammarth (Tunisia), a poorly stratified site north of Carthage (Fig. 1). The aim is to reconstruct construction dynamics and material variability through the chemical and molecular characterization of mortars, contributing new evidence to the study of Punic and early Roman building practices in North Africa.

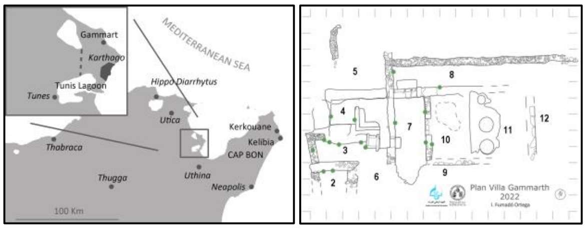

Fig. 1. Location of Gammarth (left), and plan of the archaeological site with indication of the sampling places (green dots) and enumeration of architectural defined spaces (IFO; right).

II. ARCHAEOLOGICAL BACKGROUND

The Villa of Gammarth is an archaeological site located about 6 km north of the ancient city of Carthage (Tunis, Fig. 1), which presents a series of emerging architectural structures, mainly walls and pavements from an undetermined period, in an area of little more than 100 m2 of land. These remains were discovered and rescued from destruction during an emergency intervention by the Tunisian authorities protecting the historical and archaeological heritage at the end of the 1960s, and since then no stratigraphic excavation or systematic archaeological intervention has been carried out to characterise the precise nature of these remains. However, judging by the pottery recovered during its discovery, it has been proposed that it could be interpreted as a suburban villa from the late Punic period (3rd or 2nd centuries BC). If confirmed, this site would become a unique example of its kind, as the suburban villas currently known in North Africa do not predate the change of era and developed only under Roman rule.

This site was the subject of a diagnostic visit carried out in 2019 by a Tunisian Spanish team, within the framework of archaeological collaborations between the Institut National du Patrimoine and the Centre for Phoenician and Punic Studies, under the scientific co-direction of the University of Valencia and the Institute National du Patrimoine. In 2022 it was possible to carry out a sampling campaign of building materials, mainly rocks, and plastering and construction mortars, of which we will present the latter here. More detailed archaeological information on these projects, including the working progress on the Villa Gammarth, will be soon published by Fumadó Ortega, Ben Romdhane and colleagues [12].

III. MATERIALS AND METHODS

A. The sampling

Sixteen construction mortar samples were analyzed and collected from various sectors of Gammarth Villa (Table 1, Fig. 1).

Table 1. Samples names and provenance.

Provenance	Samples
Sector 2	VG1, VG3
Sector 3	VG7-8, VG26-27, VG50, VG52
Sector 4	VG24-25
Sector 7	VG9, VG16, VG18
Sector 8	VG21-22
Sector 10	VG19

All samples have plastering function, except for VG50, which is a masonry mortar. Most of the samples (Fig. 2) are characterised by whitish to light brownish binder and sandy aggregate. VG16 and VG18 show the presence of large lime lumps. VG24-27 present some characteristics of hydraulic mortar (i.e.: *opus signinum*) with light red binder and ceramic inclusions, though VG25 binder is closer to white.

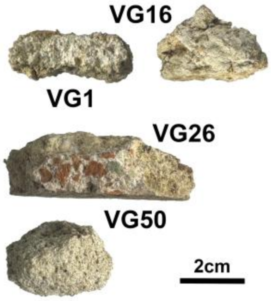

Fig. 2. Representative mortar samples for Gammarth Villa.

B. ATR-IR analysis

Each sample was cleaned with a scalpel to remove weathered surfaces and subsequently broken down using a glass mortar to remove aggregate clasts. The samples were pulverized and homogenized with an agate mortar. Infrared spectroscopy analyses have been performed by employing a Spectrum Two spectrometer by Perkin Elmer. Attenuated total reflection have been recorded for powdered samples in the 4000 to 450 cm^{-1} IR region.

C. Multielement analysis

The powdered samples were analysed by a Vanta C series Handheld pXRF spectrometer by Olympus (Waltham, MA, USA), equipped with a 40 kV rhodium anode X-ray tube and a Silicon Drift Detector (SDD). The Geochem 2-beam, used for the analyses. is characterised by 60 s of acquisition time (Beam 1: 30 s, 40 keV; Beam 2: 30 s, 10 keV). Concentration for Al, Si, S, K, Ca, Ti, Fe, and Zr were considered, being above the limits of detection in most of the samples.

The samples were also digested using aqua regia (details on the procedure are in Gallello et al. 2017 [3]) and the solutions were analyzed with a Perkin Elmer NexION 2000 ICP-MS to determine trace elements, including REE, concentrations of trace elements (Ba, Bi, Co, Cr, Cu, Li, Mo, Ni, Pb, Sr, Tl, V, Zn, Sc, Y; REE: La, Ce, Pr, Nd, Sm, Eu, Gd, Tb, Dy, Ho, Er, Tm, Yb, Lu). Certified reference materials NCS DC 73375 (Limestone) and JDo-1 (Dolostone) to evaluate data accuracy and precision.

D. Data analysis

Principal component analysis (PCA) has been carried out using data from multielement analysis and ATR-IR using R [13]. The PCA was carried out with ATR data in the region between 4000 and 250 cm -1 to identify the most relevant spectral features. Spectra were firstly processed by Savitzky-Golay filter (window = 13 points, polynomial degree = 3, derivative = 2) and mean-centered prior to the PCA. Two PCA were then carried out employing all the elements and only REE as variables respectively. In those two cases, variables were standardized prior to the analysis.

IV. RESULTS AND DISCUSSION

A. Results of ATR-IR

Data from ATR-IR were explored by the means of PCA (Fig. 3). The most relevant features were identified in the region between 1600 and 450 cm^{-1} and the first two PC explain 96.1% and 1.8% of the overall variance respectively.

The most intense loadings for both PC1 are at 872 and 712 cm^{-1}, and at 876 and 712 cm^{-1} respectively. This region is associated with vibrational modes of carbonate minerals CO_3 [14]. Loadings could thus indicate a potential shift of the first band (872-876 cm^{-1}), suggesting the presence of different types of carbonates [14, 15], or could indicate different relationship between the ~876 and ~712 cm^{-1} bands, which could be a marker of different degrees of crystallinity of calcium carbonate [16, 17]. These data would indicate possible variations in manufacturing processes or employed raw materials and recipes. Few other slight peaks can be also observed in the region between 2000 and 450 cm^{-1}.

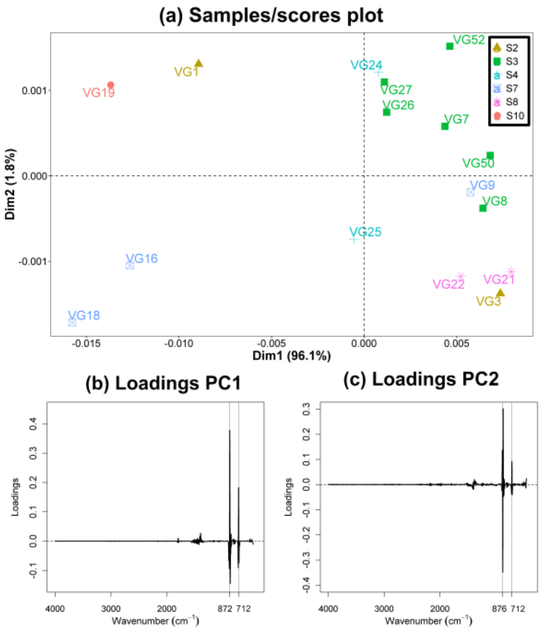

Fig. 3 Samples/scores plot for PC1 vs PC2 (a) and loadings plots for PC1 (b) and PC2 (c) for PCA of ATR-IR analysis.

Figure 4 shows representative spectra according to PCA scores. Bands at about 1795, 874 and 712 cm^{-1} are attributable to calcite [18], and they are more intense in samples with high PC1 scores (VG18-19) than in samples with low scores (VG3, VG52), and intermediate in VG24. Band peaking in the samples between 1415 and 1400 cm^{-1} is also attributable to carbonate minerals [13, 14] and its intensity follow the same trend. On the other hand, quartz and other silicate bands (1163, 1085, 1035, 1020, 850, 795, 775, 520 and 470 cm^{-1} [19-21] are stronger in the samples with negative scores. Though it was not pointed out by the PCA, it is worth noticing a combined band at 1740 cm^{-1} which is present in all the spectra except for VG24. This band could suggest the presence of organic remains, maybe from additives used for mortar manufacturing [22, 23] and it is particularly intense in VG3 and VG52. The presence of organic materials could also be responsible of the shift and the different shape of the carbonate band at ~1420 cm^{-1} in the spectra of the two cited mortars. However, more data are needed to confirm this hypothesis.

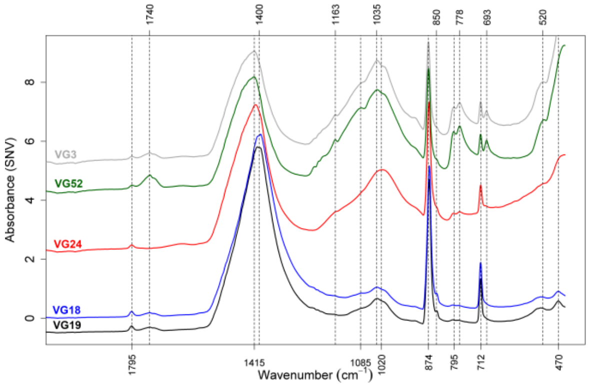

Fig. 4 Representative spectra in the 2000 to 450 cm^{-1} region. Standard normal variate (SNV) was applied and spectra were off-set to avoid overlapping.

B. Multielement analysis

Representative pXRF spectra are shown in Fig. 5. Kα and Kβ lines for Ca show the highest intensity. Differences can be seen especially related to the intensities of Ca, Si and Fe lines. Lines for Al, S, K, Ti, and Sr can also be observed most of samples. Mn line appears also in few samples.

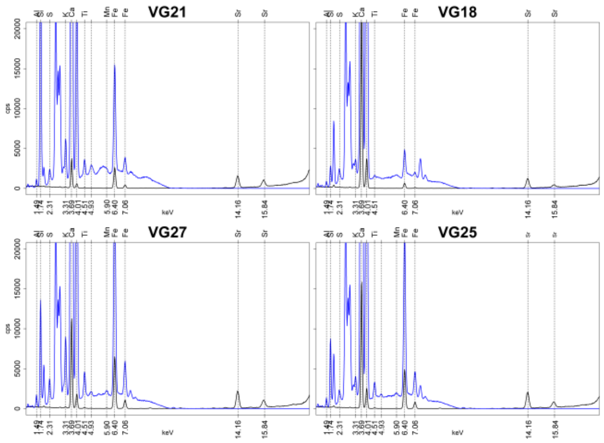

Fig. 5 Representative pXRF spectra for mortars of Gammarth villa. Black line: Beam 1 spectrum; blue line: Beam 2 spectrum; cps: counts per second.

Concentrations from multielement analyses are summarized in Table 2 (pXRF) and Table 3 (ICP-MS).

Table 2. Results of pXRF analysis.

Sector		Al	Si	S	K	Ca	Ti	Fe	Zr
S2	m	0.64	7.81	0.14	0.21	25.82	0.08	0.45	49
	s	0.68	8.36	0.14	0.18	13.16	0.03	0.16	40
S3	m	1.18	12.31	0.16	0.27	18.43	0.10	0.85	75
	s	0.78	4.75	0.07	0.10	5.50	0.07	0.70	23
S4	m	1.45	5.19	0.09	0.28	27.54	0.18	1.56	85
	s	0.25	1.35	0.08	0.21	3.61	0.03	0.14	15
S7	m	0.43	5.68	0.04	0.13	30.60	0.07	0.30	36
	s	0.22	7.61	0.04	0.04	14.58	0.02	0.07	12
S8	m	0.92	17.05	0.26	0.19	14.61	0.08	0.40	55
	s	0.45	5.92	0.15	0.13	6.47	0.02	0.22	20
S10		0.38	1.52	<LD	0.14	37.44	0.09	0.32	38

Note: Concentrations are expressed as mass percentage for Al to Si and as mg kg^{-1} for Zr. < LD = below the limit of detection; m = mean.

Table 3. Results for ICP-MS analysis.

Sector		Ba	Bi	Cd	Cr	Co	Cu	Li	Mo	Ni	Pb	Sr	Tl	V	Zn	Sc	Y	TREE
S2	m	50	0.012	0.086	6	1.448	29	2.3	0.37	2.7	12.9	297	0.016	8.2	16	0.81	2.26	14
	s	6	0.001	0.002	3	0.006	31	0.4	0.15	0.6	1.9	145	0.001	1.1	9	0.16	0.08	7
S3	m	198	0.03	0.11	18	3	89	6	0.4	8	13	277	0.03	12	15	1.4	3	22
	s	154	0.03	0.03	18	2	94	6	0.3	6	12	131	0.03	14	16	2.5	2	29
S4	m	325	0.05	0.11	40	5.3	264	13.7	0.79	13.4	31	422	0.04	33.6	33	5.7	7.6	68
	s	93	0.03	0.03	3	0.2	96	1.7	0.027	0.8	15	16	0.05	1.2	6	0.5	0.9	2
S7	m	71	0.005	0.051	4.2	1.7	6	3.0	0.31	4.4	11	248	0.022	5.5	8	0.6	1.9	9.1
	s	5	0.003	0.012	0.6	0.6	2	1.8	0.13	1.2	10	69	0.002	0.9	11	0.3	0.6	1.4
S8	m	30	0.004	0.025	6	1.2	33	3.3	0.326	3.4	9	209	0.021	8	5	0.6	1.3	12
	s	15	0.002	0.012	3	0.6	30	1.4	0.004	0.8	7	44	0.007	3.7	4	0.3	0.3	4
S10		75.5	0.009	0.047	5.01	1.98	5.54	4.54	0.446	6.52	2.80	270	0.026	6.57	<LD	0.703	1.45	9.15

Note: Concentrations are expressed as mg kg-1. < LD = below the limit of detection; TREE = sum of the REE.

PCA with all the elemental concentration permitted to identify trends relevant to understand construction practices at the site (Fig. 6). It reveals a clear differentiation among groups of mortars (Fig. 6a). PC1 and PC2 account for more than 80% of the total variance. Samples VG24-27 group separately from the others due to negative PC1 scores. These samples show red clasts which indicate the use of materials characterized by pozzolanic activity. Along PC2-axis, on the positive sides of PC1, three clusters can be observed. The first group consists of VG1, VG16 and VG18-19 characterized by PC2 negative scores; VG8-9, VG22 and VG50 form the second group, characterized by intermediate PC2 scores. Group 3 is composed by VG3, VG7, VG21 and VG52. PC1 loadings (Fig. 6b) suggest that samples characterised by negative scores are richer in most of the elements except for Si, and S and Ca. On the other hand, the most relevant variables of PC2 in the positive directions are Al, Si, S, K and Zr, and Ca in the negative direction (Fig. 5c).

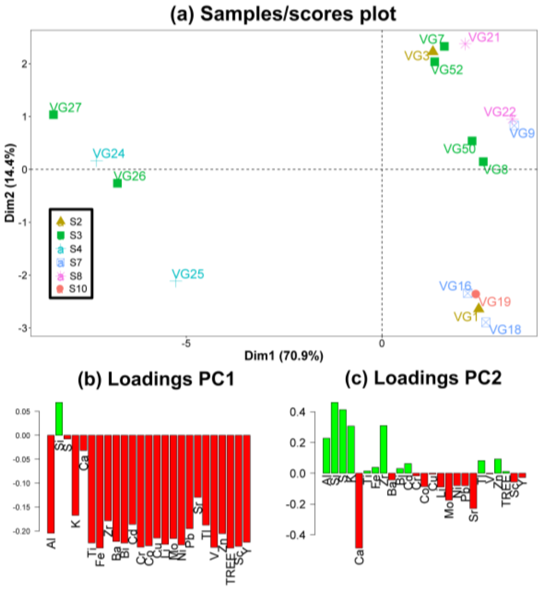

Fig. 6. Samples/scores plot (a) and loadings plots (b-c) for PCA of all the elemental concentrations.

PCA results for REE are shown in Fig. 7. The first two PCs explain 99.9% of the overall variance in the dataset. Samples/scores plot suggest the presence of at least two grouping along PC1. As for the PCA with all the elements, VG24-27 group separately due to their high PC1 scores, while the other samples are characterised by negative scores. The loadings for PC1 (Fig. 7b) suggests that the above-quoted group of samples is characterised by higher levels of lanthanides, which are positively correlated to this PC.

PC2 scores permit other interesting insights. First, VG25 has very high scores compared to the other samples of the same group which confirm the difference pointed out also by the PCA with all the elements (Fig. 6a). Furthermore, VG8-9 and VG50 have higher scores compared to the other samples on the negative side of PC1. Loadings for PC2 (Fig. 6c) indicate that scores are driven by REE fractionation given that lighter REE (La-Tb) are characterised by negative coefficients, while heavier REE (Dy-Lu) are instead characterised by positive ones. This fact possibly points out the use of different raw materials or recipes for mortar manufacturing.

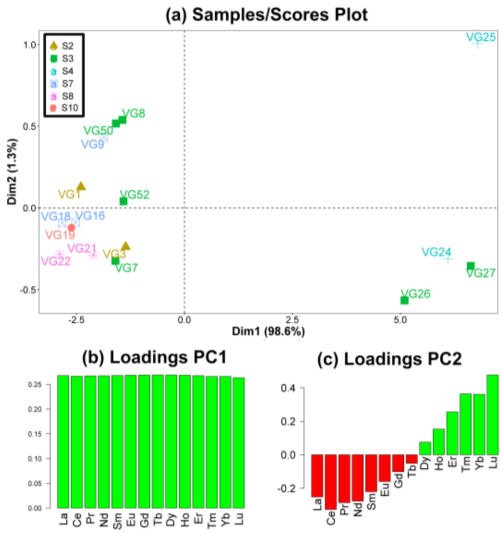

Fig. 7. Samples/scores (a) and loadings plots (b-c) for PCA of REE concentrations.

V. CONCLUSION

The multianalytical study carried out on the mortars from the archaeological complex of Gammarth Villa permitted to evidence the presence of groups of samples based on functional aspects. From this point of view, the most relevant difference is between a group of samples rich in most of the elements, including REE and the others. Macroscopic features of the former possibly indicate the addition of pozzolanic, which would be consistent with their macroscopic features and location. However, chemical data pointed out difference also among samples with similar functions. One of the possible hydraulic mortars, recognized due to their macroscopic features, also shows a distinct elemental profile, suggesting the use of different raw materials or recipes.

A following step for this research would be to widen the sample set and to perform further analyses, which include a more in-depth study of the organic phases, as well as petrographic analysis and the chemical characterisation of separated mortar phases to better understand raw material features, their potential provenance and their contribution to the chemical profile of the mortars.

VI. ACKNOWLEDGEMENTS

The collaboration has been supported by the following public projects: *Cartago y su territorio. Del ‘rst púnico al pagus Zeugei, paisajes económicos y organización territorial* (PGC2018-095280-A-100), by *Caracterización arqueométrica de la ocupación del suelo en la periferia púnica de Cartago (Túnez): la Villa de Gammart* (BBAA2019-01), by *Cartago y su territorio* (Fundación Palarq) and by PID2022-139214NB-I00 founded by MCIN/AEI/10.13039/501100011033 and by “*FEDER*

Una manera de hacer Europa, UE". MR benefits of an APOSTD postdoctoral contract (CIAPOS/2023/115) funded by Valencian Government and European Social Fund Plus (FSE+). GG is grateful to the Spanish Ministry of Science and Innovation for funding EvolMED project "Evolutionary cultural patterns in the contexts of the neolithization process in the Western Mediterranean" (PID2021-127731NB-C21). AMR thanks the Ministry of Education, Culture, Universities and Occupation of the Valencian Government which funded the Prometeo project "Smart Chemical Lab" (CIPROM/2023/37).

VII. REFERENCES

[1] A. Moropoulou, A. Bakolas, S. Anagnostopoulou, "Composite materials in ancient structures", Cement and concrete composites, vol. 27, No. 2, 2005, pp. 295-300.

[2] M. Drdácký, F. Fratini, D. Frankeová, Z. Slížková, "The Roman mortars used in the construction of the Ponte di Augusto (Narni, Italy)–A comprehensive assessment", Construction and building materials, vol. 38, 2013, pp. 1117-1128.

[3] M. Lezzerini, S. Legnaioli, G. Lorenzetti, V. Palleschi, M. Tamponi, "Characterization of historical mortars from the bell tower of St. Nicholas church (Pisa, Italy)", Construction and Building Materials, vol. 69, 2014, pp. 203-212.

[4] M.M.N. Franceschini, S. Calandra, S. Vettori, T. Ismaelli, G. Scardozzi, M.P. Caggia, E. Cantisani, "Mortars in the Archaeological Site of Hierapolis of Phrygia (Denizli, Turkey) from Imperial to Byzantine Age", Minerals, vol. 14, No. 11, 2024, 1143.

[5] G. Gallello, M. Ramacciotti, M. Lezzerini, E. Hernandez, M. Calvo, A. Morales, A. Pastor, M. De la Guardia, "Indirect chronology method employing rare earth elements to identify Sagunto Castle mortar construction periods", Microchemical Journal, vol. 132, 2017, pp. 251-261.

[6] M. Ramacciotti, S. Rubio, G. Gallello, M. Lezzerini, S.Columbu, E. Hernandez, A. Morales-Rubio, A. Pastor, M. De la Guardia, "Chronological classification of ancient mortars employing spectroscopy and spectrometry techniques: Sagunto (Valencia, Spain) Case", Journal of Spectroscopy, vol. 2018, No. 1, 2018, 9736547.

[7] L. Regev, K.M. Poduska, L. Addadi, S. Weiner, E. & Boaretto, "Distinguishing between calcites formed by different mechanisms using infrared spectrometry: archaeological applications", Journal of Archaeological Science, vol. 37, No. 12, 2010, pp. 3022-3029.

[8] M.B. Toffolo, L. Regev, S. Dubernet, Y. Lefrais, E. Boaretto, "FTIR-based crystallinity assessment of aragonite–calcite mixtures in archaeological lime binders altered by diagenesis", Minerals, vol. 9, No. 2, 2019, 121.

[9] S. Boularand, M. Turci, P. Bromblet. (2022, September), "Mineral, Chemical and Petrographic Characterization of Hydraulic Mortars & Chronological Building Correlation of the Baths of Porta Marina in Ostia Antica (Italy)", in: V. Bokan Bosiljkov, A. Padovnik, T. Turk (eds), "Conservation and Restoration of Historic Mortars and Masonry Structures", Springer Nature, Cham, Switzerland, 2022, pp. 82-96.

[10] S. Columbu, M. Palomba, F. Sitzia, M.R. Murgia, "Geochemical, mineral-petrographic and physical-mechanical characterization of stones and mortars from the Romanesque Saccargia Basilica (Sardinia, Italy) to define their origin and alteration", Italian Journal of Geosciences, vol. 137, No. 3, 2018, pp. 369-395.

[11] M. Ramacciotti, G. Gallello, M. Lezzerini, S., Pagnotta, A. Aquino, Ll. Alapont, J.A. Martín Ruiz, A. Pérez-Malumbres Landa, R. Hiraldo-Aguilera, D. Godoy Ruiz, A. Morales Rubio, M.L. Cervera, A. Pastor, "Smartphone application for ancient mortars identification developed by a multi-analytical approach", Journal of Archaeological Science: Reports, vol. 43, 2022, 103433.

[12] I. Fumadó Ortega, H. Ben Romdhane et al, "La formation du paysage carthaginois: un projet archéologique tuniso-espagnol", in I. Fumadó Ortega, H. Ben Romdhane, D. Quixal Santos (eds), "La formación del paisaje cartaginés: proyectos, ejemplos y comparaciones", Spal Monografías Arqueología, Sevilla, Spain, in press.

[13] R Core Team, "R: A Language and Environment for Statistical Computing" R Foundation for Statistical Computing, Vienna, Austria, 2024, https://www.R-project.org/

[14] V.J. Bruckman, K. Wriessnig, "Improved soil carbonate determination by FT-IR and X-ray analysis", Environmental chemistry letters, vol. 11, 2013, pp. 65-70.

[15] D. Chakrabarty, S. Mahapatra, "Aragonite crystals with unconventional morphologies", Journal of materials chemistry, vol. 9, No. 11, 1999, 2953-2957.

[16] R. Gueta, A. Natan, L. Addadi, S. Weiner, K. Refson, L. Kronik, "Local atomic order and infrared spectra of biogenic calcite", Angewandte Chemie-International Edition, vol. 46, No. 1-2, 2007, pp. 291-294.

[17] V. Kotlyar, "The Calcite Crystallinity and the Age of Limestone Brick Mortars of Medieval Objects of the North of the Byzantine Oecumene", in Materials Science Forum, Vol. 974, 1999, pp. 83-89.

[18] V.J. Bruckman, K. Wriessnig, "Improved soil carbonate determination by FT-IR and X-ray analysis", Environmental chemistry letters, vol. 11, 2013, pp. 65-70.

[19] G. Parthasarathy, A.C. Kunwar, R. Srinivasan, "Occurrence of moganite-rich chalcedony in Deccan flood basalts, Killari, Maharashtra, India", European Journal of

Mineralogy, vol. 13, No. 1, 2001, pp. 127-134.

[20] D.A. Silva, H. R. Wenk, P.J.M. Monteiro, "Comparative investigation of mortars from Roman Colosseum and cistern", Thermochimica Acta, vol. 438, No. 1-2, 2005, pp. 35-40.

[21] J.J.V.S. Madejová, "FTIR techniques in clay mineral studies", Vibrational spectroscopy, vol. 31, No. 1, 2003, pp. 1-10.

[22] P. Bauerová, M. Kracík-Štorkánová, P. Mácová, P. Reiterman, E. Vejmelková, M. Keppert, "Estimation of the linseed oil content in historic lime mortar", Journal of Thermal Analysis and Calorimetry, vol. 148, No. 3, 2023, pp. 697-709.

[23] L. Rampazzi, M.P. Colombini, C. Conti, C. Corti, A. Lluveras‐Tenorio, A. Sansonetti, M. Zanaboni, "Technology of medieval mortars: an investigation into the use of organic additives", Archaeometry, vol. 58, No. 1, 2016, pp. 115-130.